1521-0103/368/1/21–31$35.00
THE JOURNAL OF PHARMACOLOGY AND EXPERIMENTAL THERAPEUTICS

https://doi.org/10.1124/jpet.118.254045
J Pharmacol Exp Ther 368:21–31, January 2019

The Journal of PHARMACOLOGY And Experimental Therapeutics

Pharmacological Inhibition of the Temperature-Sensitive and Ca^{2+}-Permeable Transient Receptor Potential Vanilloid TRPV3 Channel by Natural Forsythoside B Attenuates Pruritus and Cytotoxicity of Keratinocytes

Heng Zhang,[1] Xiaoying Sun,[1] Hang Qi, Qingxia Ma, Qiqi Zhou, Wei Wang, and KeWei Wang

Department of Pharmacology, School of Pharmacy, Qingdao University, Qingdao, China

Received September 27, 2018; accepted October 26, 2018

ABSTRACT

The temperature-sensitive and calcium-permeable transient receptor potential vanilloid 3 (TRPV3) channel abundantly expressed in keratinocytes plays important functions in skin physiology. Dysfunctional gain-of-function *TRPV3* gene mutations cause genetic Olmsted syndrome characterized by periorificial keratoderma, palmoplantar keratoderma, inflammation, and severe itching, which suggests that pharmacological inhibition of overactive TRPV3 function may be beneficial in treating pruritus or skin disorders. To test this hypothesis, we identified natural compound forsythoside B as a TRPV3 inhibitor through screening of human embryonic kidney 293 (HEK293) cells expressing human TRPV3 channels in a calcium fluorescent assay. Whole-cell patch-clamp recordings of HEK293 cells expressing TRPV3 confirmed that forsythoside B selectively inhibited the channel current activated by agonist 2-aminoethoxydiphenyl borate (50 μM) in a dose-dependent fashion, with an IC_{50} value of 6.7 $\pm$ 0.7 μM. In vivo evaluation of scratching behavior demonstrated that pharmacological inhibition of TRPV3 by forsythoside B significantly attenuated acute itch induced by either the TRPV3 agonist carvacrol or the pruritogen histamine, as well as chronic itch induced by acetone-ether-water in a mouse model of dry skin. Furthermore, forsythoside B was able to prevent the death of HEK293 cells or native human immortalized nontumorigenic keratinocyte cells from human keratinocytes expressing a gain-of-function TRPV3 G573S mutant or in the presence of the TRPV3 agonist carvacrol. Taken together, our findings demonstrate the crucial role of TRPV3 in pruritus and keratinocyte toxicity; thus, specific inhibition of overactive TRPV3 by natural forsythoside B may possess therapeutic potential for treatment of chronic pruritus, skin allergy, or inflammation-related skin diseases.

Introduction

The warm temperature–activated and calcium-permeable nonselective cation transient receptor potential vanilloid 3 (TRPV3) channel is most abundantly expressed in skin keratinocytes and plays a crucial role in numerous physiologic processes such as cutaneous sensation, hair growth, and skin barrier formation (Cheng et al., 2010; Aijima et al., 2015). TRPV3 channel dysfunction caused by genetic gain-of-function mutations or pharmacological activation is implicated in the pathogenesis of skin inflammation, dermatitis, and chronic itch (Asakawa et al., 2006; Imura et al., 2009; Lin et al., 2012; Cui et al., 2018). In rodents, a spontaneous gain-of-function mutation of the *TRPV3* gene in WBN/Kob-Ht rats (Gly573 substituted by Cys) and DS-*Nh* mice (Gly573 substituted by Ser) causes the development of skin lesions with pruritus and dermatitis (Asakawa et al., 2006; Imura et al., 2009; Yoshioka et al., 2009; Yamamoto-Kasai et al., 2013), and silencing of TRPV3 attenuates itch sensation or inflammatory pain (Bang et al., 2012; Yamamoto-Kasai et al., 2012; Sun et al., 2018). We previously reported three gain-of-function mutations of TRPV3 (W692G, G573C, and G573S) in Chinese patients with genetic Olmsted syndrome (OS) featured with mutilating palmoplantar keratoderma with dermatitis, periorificial keratotic plagues, and severe itching (Lin et al., 2012). Inside-out or whole-cell patch-clamp recordings demonstrate that these TRPV3 mutants are constitutively open, with robust inward currents (Xiao et al., 2008; Lin et al., 2012) and elevation of intracellular

This work was supported by the Ministry of Science and Technology of China [Grant 2014ZX09507003-006-004 (to K.W.)], the Natural Science Foundation of China [Grant 81573410 (to K.W.)], the Natural Science Foundation of Shandong Province [Grant ZR2017BH020 (to X.S.)], and the Qingdao Postdoctoral Application Research Project [Grant 2015154 (to X.S.)].
[1]H.Z. and X.S. contributed equally to this work.
https://doi.org/10.1124/jpet.118.254045.

ABBREVIATIONS: 2-APB, 2-aminoethoxydiphenyl borate; AEW, acetone-ether-water; DMSO, dimethylsulfoxide; GSK1016790A, (*N*-((1*S*)-1-{[4-((2*S*)-2-{[(2,4-dichlorophenyl)sulfonyl]amino}-3-hydroxypropanoyl)-1-piperazinyl]carbonyl}-3-methylbutyl)-1-benzothiophene-2-carboxamide; HaCaT, human immortalized nontumorigenic keratinocyte; HEK293, human embryonic kidney 293; NF-κB, nuclear factor κB; OS, Olmsted syndrome; PI, propidium iodide; TRP, transient receptor potential; TRPA, transient receptor potential ankyrin; TRPV, transient receptor potential vanilloid; WT, wild type.

Ca^{2+} that subsequently triggers keratinocyte cell death (Lin et al., 2012). Similar gain-of-function TRPV3 mutations were also reported in studies from other countries, which were performed in patients with OS characterized by dermatitis and severe itching (Duchatelet et al., 2014; Eytan et al., 2014; Kariminejad et al., 2014; Choi et al., 2018). These observations demonstrate that TRPV3 has emerged as a promising therapeutic target, and specific inhibition of overactive TRPV3 may present therapeutic potential for the treatment of chronic pruritus or skin diseases, which is a currently unmet medical need.

As a polymodal sensor, ligand-gated TRPV3 is also activated by a number of chemicals, including 2-aminoethoxydiphenyl borate (2-APB), intracellular protons, endogenous ligand farnesyl pyrophosphate, and natural compounds such as carvacrol, thymol, and camphor (Chung et al., 2004; Xu et al., 2006; Bang et al., 2010; Cao et al., 2012; Cui et al., 2018). TRPV3 is also inhibited by 2,2-diphenyltetrahydrofuran (a 2-APB structural analog; Chung et al., 2005), isopentenyl pyrophosphate (Bang et al., 2011), 17(*R*)-resolvin D1 (an anti-inflammatory lipid mediator; Bang et al., 2012), icilin (a transient receptor potential melastatin TRPM8 and transient receptor potential ankyrin TRPA1 channel agonist; Sherkheli et al., 2012), Mg^{2+} (Luo et al., 2012), and ruthenium red (a broad-spectrum TRP channel inhibitor; Nilius et al., 2007). However, there is a lack of selective TRPV3 antagonists, which hampers the pharmacological study of TRPV3 channel function. Thus, it is imperative to discover specific TRPV3 inhibitors that can be used to validate TRPV3 as a therapeutic target and to treat skin diseases associated with overactive TRPV3 function.

Lamiophlomis rotata, also known as Tibetan Duyiwei, is grown in Tibet and Southwestern areas of China and is commonly used as a traditional Chinese herbal medicine to alleviate detumescence, inflammation, and pain (Jiang et al., 2010a; Zhu et al., 2014). As an active ingredient of *L. rotata* leaves, forsythoside B is a phenylethanoid glycoside that suppresses inflammatory responses via inhibition of nuclear factor κB (NF-κB) signaling (Jiang et al., 2010a,b, 2012). A recent study also demonstrated that activation of TRPV3 induces the inflammatory response mediated by NF-κB signaling (Szöllősi et al., 2018). Based on these investigations, we hypothesized that forsythoside B might act as an inhibitor of TRPV3.

In this study, we used a calcium influx fluorescent assay and found that natural compound forsythoside B was able to specifically inhibit TRPV3 channel activity in a dose-dependent fashion. In vivo evaluation demonstrated that forsythoside B exerted antipruritic effects on acute itch induced by the TRPV3 agonist carvacrol or by the pruritogen histamine, as well as chronic itch induced by acetone-ether-water (AEW) in a mouse model of dry skin. Forsythoside B also prevented cell death triggered by TRPV3 gain-of-function mutation or agonist carvacrol in either human embryonic kidney 293 (HEK293) cells expressing TRPV3 channels or in native human immortalized nontumorigenic keratinocyte (HaCaT) cells from a human skin keratinocyte cell line. Our findings demonstrate that specific inhibition of TRPV3 by natural compound forsythoside B attenuates pruritus and keratinocyte cell death, suggesting the therapeutic potential of forsythoside B for the treatment of chronic pruritus, dermatitis, or inflammation-related skin diseases.

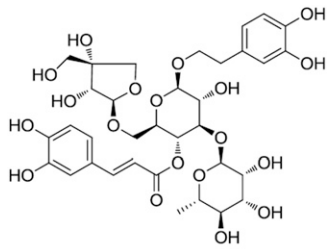

Fig. 1. Chemical structure of natural compound forsythoside B.

Materials and Methods

Reagents and Compounds. Natural compound forsythoside B, with a molecular mass of 756.7 g/mol and purity greater than 99%, was obtained from Taoto Biotech Corporation Ltd. (Shanghai, China). The chemical structure of forsythoside B is shown in Fig. 1. TRPV3 agonists 2-APB and carvacrol, TRPV1 agonist capsaicin, TRPA1 agonist allyl isothiocyanate, TRPV4 agonist GSK1016790A [(*N*-((1*S*)-1-{[4-((2*S*)-2-{[(2,4-dichlorophenyl)sulfonyl]amino}-3-hydroxypropanoyl)-1-piperazinyl]carbonyl}-3-methylbutyl)-1-benzothiophene-2-carboxamide], and TRP channel antagonist ruthenium red were obtained from Sigma-Aldrich (St. Louis, MO). Reports of high-performance liquid chromatography analyses of these standard compounds indicate a compound purity of no less than 98.0%. With the exception of ruthenium red dissolved in water, stock solutions of forsythoside B (100 mM), GSK1016790A (500 μM), and 2-APB (1 M) were prepared in dimethylsulfoxide (DMSO). The final DMSO concentration in each compound solution did not exceed 0.2%. The stock solution of capsaicin (100 mM) was prepared in absolute ethanol. Compounds used for the measurement of intracellular fluorescent calcium were diluted in Hanks' balanced salt solution. For whole-cell patch-clamp recordings, all compounds were prepared in perfusion solution. With the exception of carvacrol dissolved in 10% ethanol, the compounds used in the evaluation of scratching behaviors were diluted in normal saline.

Animals. C57BL/6 male mice aged 6–8 weeks were purchased from Vital River Laboratory Animal Technology Co. Ltd. (Beijing, China). Evaluation of pruritic scratching behavior was carried out after mice were acclimatized to their housing environment for at least 7 days. Mice were housed and maintained in an environment with a 12-hour/12-hour light/dark cycle and a controlled temperature of 22.0 ± 2.0°C. Mouse food and water were accessible ad libitum. All experimental protocols for animals were approved by the Qingdao University Institutional Animal Care and Use Committee. All in vivo experiments were carried out in compliance with national and institutional guidelines for the care and use of laboratory animals.

Cell Culture. HEK293 and HaCaT cells were cultured in Dulbecco's minimal essential medium supplemented with 10% fetal bovine serum at 37°C with 5% CO_2. HEK293 cells were seeded in a 12-well plate for intracellular calcium measurement. For whole-cell patch-clamp recordings, HEK293 cells were cultured on glass coverslips. HEK293 cells were transiently transfected with individual cDNA plasmids of hTRPV3, hTRPV1, hTRPV4, and hTRPA1 using Lipofectamine 2000 (Invitrogen, Carlsbad, CA). To identify transfected cells, all plasmids were tagged with green fluorescent protein for whole-cell patch-clamp recordings. Human TRPV3 plasmids including wild-type (WT) or mutant G573S were described previously (Lin et al., 2012), and the correct TRPV3 mutation was verified by DNA sequencing.

Measurement of Intracellular Fluorescent Calcium in the FlexStation 3 Assay. The Cal-520 PBX Calcium Assay Kit (AAT Bioquest, Sunnyvale, CA) was used to detect the change in intracellular calcium ($[Ca^{2+}]_i$) in a population of cells using a multimode

microplate reader in a FlexStation 3 assay (Molecular Devices, San Jose, CA). HEK293 cells were transfected with cDNAs of TRP channels before they were seeded at a density of approximately 40,000 cells per well in a 96-well black-walled plate (Thermo Fisher Scientific, Waltham, MA) for overnight culture at 37°C with 5% CO_2. To measure intracellular calcium, cells were incubated with the calcium fluorescent dye provided in the Cal-520 PBX Calcium Assay Kit at 37°C for 1.5 hours; relative fluorescence units were measured in the FlexStation 3 assay under an excitation wavelength at 485 nm and an emission wavelength at 515 nm at an interval of 1.6 seconds (Sun et al., 2018).

Electrophysiology. Whole-cell patch-clamp recordings were carried out using an EPC10 amplifier driven by PatchMaster software (HEKA, Instrument Inc, Lambrecht/Pfalz, Germany). The borosilicate glass pipette was pulled using a DMZ-Universal puller (Zeitz Instruments GmbH, Martinsried, Germany) and was fire polished to a resistance of 3 to 4 MΩ. Both bath solution and pipette solution used for whole-cell recordings contained 130 mM NaCl, 3 mM HEPES, and 0.2 mM EDTA, with the pH adjusted at 7.2 (Wei et al., 2016). TRP channel current was recorded in cells held at 0 mV in response to a voltage ramp from −100 to +100 mV for 500 milliseconds, and the current was analyzed at ±80 mV. Origin 8.6 software (OriginLab, Northampton, MA) was used to analyze the data.

Evaluation of Pruritic Scratching Behavior. To assess itch-scratching behavior, an electric hair clipper was used to shave the hair on the right side of the rostral part of the mouse neck 24 hours before the start of experiments. Scratching behavior was recorded on video. The number of itch-scratching bouts was counted through video playback analysis. One scratching bout was counted when a mouse raised its right hindlimb to the injection site and continuously scratched for any time length before it returned the limb to its mouth or the floor (Wilson et al., 2013). All behavioral experiments were conducted in a double-blind manner (Sun et al., 2018).

In order to test acute itch induced by TRPV3 agonist carvacrol or pruritogen histamine, mice were put in an observation box (length, width, and height: 9 × 9 × 13 cm^3) for acclimatization for about 30 minutes. Then 50 μl carvacrol (0.1%) or histamine (100 μM) was injected intradermally into the right side of the mouse neck. To access the effect of forsythoside B on itch scratching, vehicle (0.3% DMSO) or forsythoside B (3, 30, and 300 μM) was injected intradermally 30 minutes before intradermal injection of the agonist carvacrol. For video recordings of acute itch induced by histamine, vehicle (0.03% DMSO) or forsythoside B (0.3, 3, or 30 μM) was injected intradermally 30 minutes before intradermal injection of 100 μM pruritogen histamine (Cui et al., 2018; Sun et al., 2018).

To assess AEW-induced dry skin and chronic itch, the bare skin on the right side of the mouse nape was smeared with an acetone and ether (1:1) mixture or water for 15 seconds, followed by water treatment for 30 seconds, for a period of 5 days (Miyamoto et al., 2002; Yamamoto-Kasai et al., 2012). On day 6, the mouse was placed in an observation box (length, width, and height: 9 × 9 × 13 cm) for acclimatization for about 30 minutes. Different concentrations of forsythoside B (0.3, 3, or 30 μM) or 0.03% DMSO vehicle were injected intradermally into the right side of the mouse nape in 50 μl of total volume, and scratching was recorded on video for 60 minutes after intradermal injection of forsythoside B.

In order to test locomotor activity, a mouse was observed in an open-field chamber with built-in infrared photoelectric sensors after intradermal injection of 50 μl forsythoside B (0.3, 3, 30, and 300 μM) into the right side of the neck. Locomotor activity as the total distance traveled in the open-field chamber was analyzed for 60 minutes.

Cell Death Assay. HEK293 cells or HaCaT cells from a human skin cell line were seeded in six-well plates and randomly divided into different groups. After administration of compounds for 12 hours, cell death was determined by labeling with Hoechst 33258 dye (Thermo Fisher Scientific) for all cell nuclei or with propidium iodide (PI) dye (Thermo Fisher Scientific) for the nuclei of dead cells. In each group, five images were randomly taken under a microscope (Eclipse Ti; Nikon, Tokyo, Japan) and automatically counted on a confocal microscope (A1R MP; Nikon). The cell death ratio was represented by the average of PI-labeled cells over Hoechst-labeled cells from five images. Because the transfection ratio maintained for the WT TRPV3 or G573S TRPV3 mutant was low at about 22.47% ± 1.56% at 12 hours in HEK293 cells, the cell death ratio was normalized in mutant G573S-induced cell death in HEK293 cells.

Statistical Analysis. All data are expressed as means ± S.E.M. The *t* test (two-tailed, unpaired) or one-way analysis of variance with GraphPad Prism 7.0 software (GraphPad Inc., La Jolla, CA) was used to analyze the statistical significance ($P < 0.05$, $P < 0.01$, $P < 0.001$, $P < 0.0001$). IC_{50} values were determined by the half maximal inhibitory concentration of the tested compounds.

Molecular Docking. Docking calculations were completed using the AutoDock 4.2 program (Morris et al., 1998). The three-dimensional structure of forsythoside B was generated by the PRODRG2 server (Schüttelkopf and van Aalten, 2004). AutoDockTools software was used to convert the structure of forsythoside B into AutoDock 4.2 format for docking to the structure of TRPV3 channel protein (Protein Data Bank code 6DVW) (Singh et al., 2018). Because TRPV3 is composed of four identical subunits, one subunit was used to dock the forsythoside B compound. For each atom of the macromolecules, Gasteiger charges were calculated and an electrostatic map and a desolvation map were computed by AutoDock 4.2. The Lamarckian genetic algorithm was used in the docking simulation for ligand conformational searching according to the standard protocol. All figures of structural models were generated by PyMOL (https://pymol.org/; Schrödinger, New York, NY).

Results

Identification of Natural Compound Forsythoside B as a TRPV3 Inhibitor. We started screening for the inhibitory effect of compounds on an increase in intracellular calcium caused by activating hTRPV3 channels transiently expressed in HEK293 cells in a calcium fluorescent assay using a FlexStation 3 multimode microplate reader. Each compound was added to a well of a 96-well black-walled plate at 17 seconds before the addition of TRPV3 agonist 2-APB at 100 seconds. Relative fluorescence units were measured for another 80 seconds. The addition of forsythoside B reduced the intracellular Ca^{2+} influx caused by 200 μM 2-APB in HEK293 cells expressing hTRPV3 channels (Fig. 2A). Increasing forsythoside B concentrations (50, 100, and 200 μM) dose-dependently reduced the intracellular Ca^{2+} influx mediated by activation of TRPV3 channels compared with 50 μM ruthenium red, a broad-spectrum TRP channel blocker.

To confirm the inhibition of TRPV3 current by forsythoside B, we carried out whole-cell patch-clamp recordings of HEK293 cells expressing TRPV3 channels. Perfusion of 50 μM forsythoside B significantly reduced the channel current elicited by 50 μM 2-APB about 81.5% ± 6.8% (Fig. 2B). Increasing different concentrations (1–100 μM) of forsythoside B caused dose-dependent inhibition of TRPV3 channel current, with an IC_{50} value of 6.7 ± 0.7 μM (Fig. 2C). These results indicate that forsythoside B inhibits TRPV3-mediated Ca^{2+} influx or TRPV3 current induced by agonist 2-APB.

Selective Inhibition of TRPV3 Channel Current by Forsythoside B. To determine the selectivity of forsythoside B, we examined the effects of forsythoside B on other thermo-TRP channels previously reported to be involved in itch signaling, such as TRPV1, TRPV4, and TRPA1 (Zhang, 2015; Chen et al., 2016). The channel currents were activated by a voltage ramp from −100 to +100 mV for 500 milliseconds.

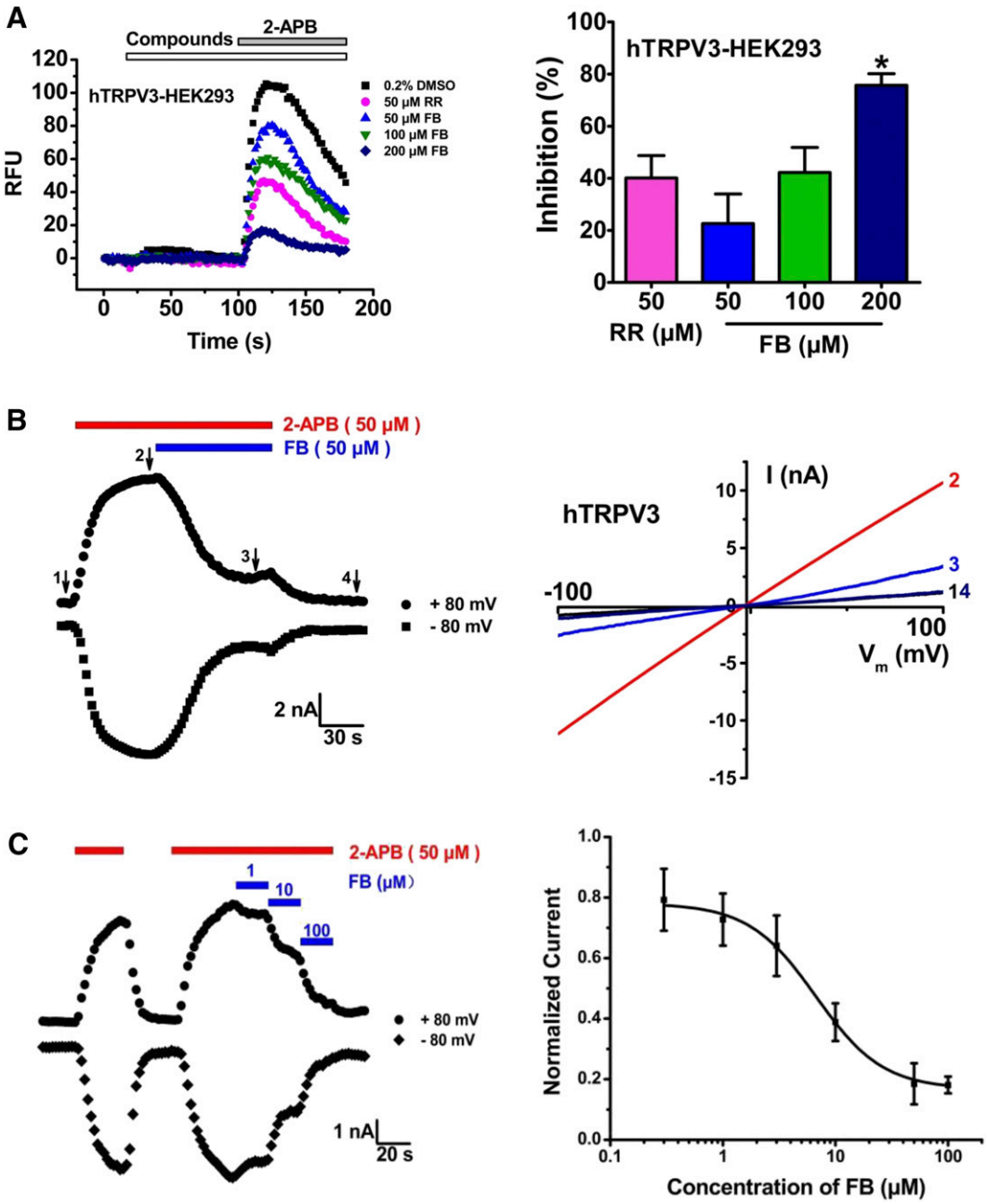

Fig. 2. Identification of natural forsythoside B as an inhibitor of hTRPV3 channels expressed in HEK-293 cells. (A) Dose-dependent inhibition of intracellular Ca^{2+} increase mediated through activation of TRPV3 channels in response to 200 μM 2-APB by different concentrations of forsythoside B ranging from 50 to 200 μM in a FlexStation 3 calcium fluorescent assay. The right panel shows a summary of the inhibition of the intracellular fluorescent Ca^{2+} increase shown in the left panel. The blank control is 0.2% DMSO. Asterisks denote statistical significance compared with the ruthenium red control ($n = 6$; $^*P < 0.05$, by one-way analysis of variance). (B) Whole-cell patch-clamp recordings of TRPV3 currents in response to 2-APB alone (50 μM, red bar) or coapplication of 50 μM forsythoside B (blue bar). The right panel shows current-voltage curves of hTRPV3 in response to voltage ramps from −100 to +100 mV before (1) and after 50 μM 2-APB (2), after the coaddition of 50 μM 2-APB and 50 μM forsythoside B (3), and after washout (4). (C) The left panel shows the representative hTRPV3 currents in response to 50 μM 2-APB before and after its coaddition with increasing concentrations of forsythoside B (from 1 to 100 μM). The right panel shows curve fitting of dose-dependent inhibition of 2-APB–mediated hTRPV3 activation by forsythoside B, with an IC_{50} of 6.7 ± 0.7 μM (n = 5–10). Data are presented as means ± S.E.M. FB, forsythoside B; RFU, relative fluorescence unit; RR, ruthenium red.

Perfusion of forsythoside B (50 μM) had only a slight reduction of about 12.1% ± 3.7% of TRPV1 current induced by 1 μM of selective agonist capsaicin (Fig. 3, A and D), about 14.8% ± 4.9% of TRPV4 current induced by 50 nM of selective agonist GSK1016790A (Fig. 3, B and D), or about 10.9% ± 4.5% of TRPA1 channel current evoked by 300 μM allyl isothiocyanate (Fig. 3, C and D) compared with 81.5% inhibition of TRPV3 current by forsythoside B (50 μM). These data indicate the selective inhibition of TRPV3 by natural compound forsythoside B over other thermo-TRP channels such as TRPV1, TRPV4, and TRPA1.

Forsythoside B Suppresses Acute Itch Induced by the Pruritogen Carvacrol or Histamine. Our recent observations show that pharmacological activation of the

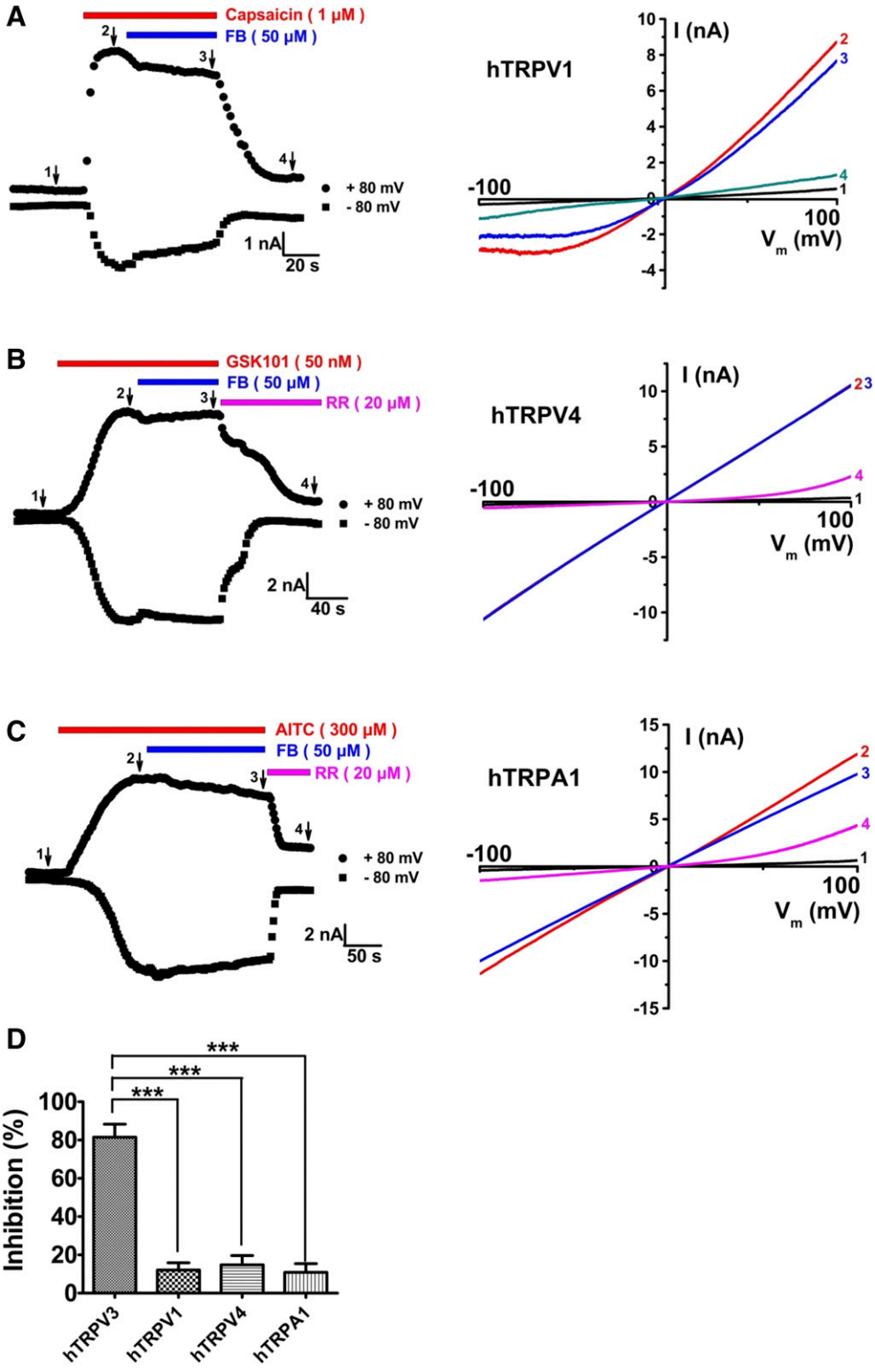

Fig. 3. Selective inhibition of TRPV3 current by forsythoside B over TRPV1, TRPV4, and TRPA1 channels. (A) Representative hTRPV1 current activated by 1 μM capsaicin (red bar) before and after its coapplication with 50 μM forsythoside B (blue bar) and washout. The right panel shows current-voltage curves of hTRPV1 in response to voltage ramps from −100 to +100 mV shown in the left panel before (1) and after 1 μM capsaicin (2), after the coaddition of 50 μM forsythoside B and 1 μM capsaicin (3), and after washout (4). (B) Representative hTRPV4 current activated by 50 nM GSK1016790A (red bar) or in the absence or presence of 50 μM forsythoside B (blue bar) before inhibition by 20 μM ruthenium red (pink bar). The right panel shows current-voltage curves of hTRPV4 in response to voltage ramps from −100 to +100 mV shown in the left panel before (1) and after 50 nM GSK101 (2), after coaddition of 50 μM forsythoside B and 50 nM GSK101 (3), and after addition of 20 μM ruthenium red (4). (C) Representative hTRPA1 current activated by 300 μM AITC (red bar) or in the absence or presence of 50 μM forsythoside B (blue bar) before complete inhibition by 20 μM ruthenium red (pink bar). The right panel shows the current-voltage curves of hTRPA1 in response to voltage ramps from −100 to +100 mV shown in the left panel before (1) and after 300 μM AITC (2), after coaddition of 50 μM forsythoside B and 300 μM AITC (3), and after addition of 20 μM ruthenium red (4). (D) Summary of the percent inhibition of hTRPV3, hTRPV1, hTRPV4, and hTRPA1 channel activation by 50 μM forsythoside B. Data are presented as means ± S.E.M. Asterisks denote statistical significance compared with the hTRPV3 control (n = 5 to 6; ***$P < 0.001$, by unpaired t test). AITC, allyl isothiocyanate; FB, forsythoside B; GSK101, GSK1016790A; RR, ruthenium red.

TRPV3 channel by carvacrol can evoke scratching behavior in mice (Cui et al., 2018). To determine the inhibitory effect of forsythoside B on TRPV3 activation-induced itch, we made an intradermal injection of forsythoside B into the mouse neck 30 minutes before injection of carvacrol into the same site. After intradermal injection of carvacrol (0.1%), the spontaneous scratching bouts were dramatically increased about 5.7-fold to 188.9 ± 35.5 (n = 9, $P < 0.001$) from 33 ± 4.1 (n = 7) for the group administered vehicle (10% ethanol) within 30 minutes (Fig. 4A). In contrast, intradermal injection of 30 or 300 μM forsythoside B led to a dramatic decrease in scratching bouts to 83.7 ± 23.8 (n = 9, $P < 0.05$) and 45.6 ± 6.4 (n = 7, $P < 0.01$), respectively (Fig. 4A). These results indicate that forsythoside

B suppresses the scratching behavior induced by TRPV3 agonist carvacrol.

Histamine, the most common pruritogen, causes acute itch in humans and rodents (Sun and Dong, 2016). The histamine level in the skin of DS-*Nh* mice carrying a gain-of-function TRPV3 mutation is substantially higher compared with age-matched DS mice (Asakawa et al., 2006). Similarly, TRPV3 knockout mice also exhibit attenuation of pruritus evoked by histamine (Sun et al., 2018). Thus, we further tested the effect of forsythoside B on histamine-dependent acute itch evoked by histamine. As shown in Fig. 4B, intradermal injection of 100 μM histamine into the mouse nape led to a dramatic increase in spontaneous scratching behavior, with the number of bouts at 52.2 $\pm$ 6.4 within 30 minutes ($n = 6$, $P < 0.01$) compared with 3.4 $\pm$ 1.8 for the vehicle control ($n = 5$). Pretreatments with different concentrations (0.3, 3, or 30 μM) of forsythoside B significantly reduced the scratching bouts in a dose-dependent manner to 22.5 $\pm$ 7.7 ($n = 6$, $P < 0.01$), 15.5 $\pm$ 4.9 ($n = 6$, $P < 0.001$), and 5.8 $\pm$ 1.6 ($n = 6$, $P < 0.001$), respectively (Fig. 4B), indicating that forsythoside B suppresses histamine-induced scratching behavior.

Forsythoside B Attenuates Pruritic Scratching Behavior in a Mouse Model of Dry Skin. Investigations from our group and others show that dry skin induced by AEW evokes spontaneous scratching in normal mice but not TRPV3 knockout mice (Miyamoto et al., 2002; Yamamoto-Kasai et al., 2012; Sun et al., 2018). We therefore further tested the effect of TRPV3 inhibition by forsythoside B on scratching behavior in a model of dry skin induced by AEW treatment. The skin of the mouse nape became dry with white dandruff after 5-day AEW treatment compared with a vehicle control water treatment (Sun et al., 2018). On day 6, different concentrations of forsythoside B (0.3, 3, or 30 μM in 50 μl) or DMSO vehicle (0.03%) were injected intradermally into the right nape after

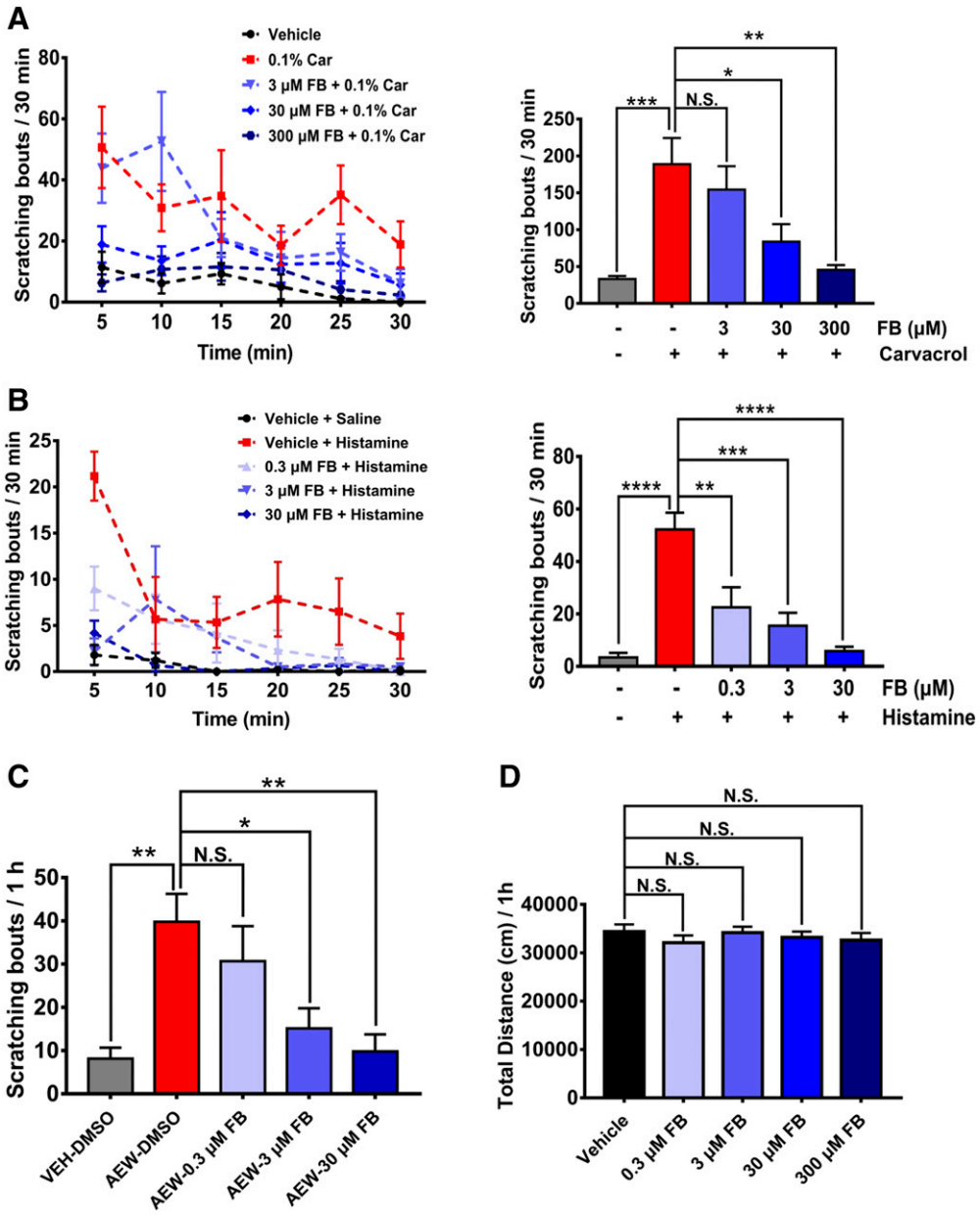

Fig. 4. Forsythoside B reduces scratching behavior induced by carvacrol and histamine or AEW in mice. (A) The left panel shows the time course of neck-scratching activity observed in C57BL/6 mice after intradermal injection of 50 μl carvacrol (0.1%) into the mouse neck, with pretreatment with vehicle (0.3% DMSO) and different concentrations (3, 30, or 300 μM) of 50 μl forsythoside B in the same site. Time for scratching bouts was plotted for each 5-minute bin over 30 minutes. The right panel shows quantification of scratching bouts during the 30 minutes shown in the left panel (n = 7–9; no significance; $^*P < 0.05$; $^{**}P < 0.01$; $^{***}P < 0.001$, by one-way ANOVA). (B) The left panel shows the representative time course of neck-scratching activity observed after intradermal injection of 50 μl histamine (100 μM) into the mouse neck, with pretreatment with vehicle (0.03% DMSO) and different concentrations (0.3, 3, or 30 μM) of 50 μl forsythoside B into the same site. Time for scratching bouts was plotted for each 5-minute bin over 30 minutes. The right panel shows the quantification of scratching bouts during the 30 minutes shown in the left panel (n = 5 to 6; no significance; $^{**}P < 0.01$; $^{***}P < 0.001$; $^{****}P < 0.0001$ by one-way ANOVA). (C) Dose-dependent inhibition of spontaneous scratching bouts in AEW-treated mice by pretreatment with topical application of forsythoside B (n = 5–9; no significance; $^*P < 0.05$; $^{**}P < 0.01$, by one-way ANOVA). (D) Locomotor activity assessment (total travel distance, in centimeters) after intradermal injection with forsythoside B (0.3, 3, 30, or 300 μM; 50 μl/site) into the nape of the mouse neck (n = 5; no significance, by one-way ANOVA). ANOVA, analysis of variance; Car, carvacrol; FB, forsythoside B; N.S., no significance.

mice were acclimatized for 30 minutes. Itch-scratching behavior was recorded on video for 60 minutes after intradermal injections. As shown in Fig. 4C, AEW treatment induced a significant increase in spontaneous scratching bouts (39.8 ± 6.4; $n = 5$, $P < 0.01$) compared with the blank control water treatment (8.1 ± 2.5; $n = 7$) within 60 minutes. In contrast, application of 3 and 30 μM forsythoside B significantly reduced itch-scratching bouts to 15.1 ± 4.6 ($n = 8$, $P < 0.05$) and 9.8 ± 4.0 ($n = 9$, $P < 0.01$), respectively.

To exclude any possible sedative effects caused by forsythoside B, locomotor activity assessment was performed after intradermal injection of different concentrations of forsythoside B into the nape of the mouse neck within 60 minutes. As shown in Fig. 4D, administration of different concentrations of forsythoside B (0.3–300 μM in 50 μl) had no significant alteration in the total distance traveled in the chambers. These results suggest that forsythoside B attenuates dry skin–induced chronic itch likely through direct inhibition of TRPV3 channel function.

Forsythoside B Attenuates Cell Death in HEK293 or HaCaT Cells Expressing the Constitutively Open TRPV3 G573S Mutant in a Dose-Dependent Manner. We previously observed that keratinocytes from keratotic skin lesions in patients with OS undergo significant apoptosis with a higher cell death ratio (Lin et al., 2012), indicating that keratinocyte cell death is characteristic of dermatitis or skin diseases. Cotransfection of WT TRPV3 with the gain-of-function G573S mutant in HEK293 cells was shown to partially rescue cell death triggered by the G573S mutant (Xiao et al., 2008), suggesting that inhibition of TRPV3 can protect against cell death caused by overactive TRPV3 function. We determined the cell death ratio by PI staining for dead cells over Hoechst staining of all cells. The normalized cell death ratio was maintained at a low level (6.78% ± 2.04%) in HEK293 cells transfected with WT TRPV3 (Fig. 5, A and B), indicating that transfection of WT TRPV3 had little effect on triggering cell death. In contrast, transfection of the TRPV3 G573S mutant significantly increased the cell death ratio to 48.61% ± 6.45%. Addition of 10 and 100 μM forsythoside B effectively reduced the cell death ratio to 26.76% ± 4.97% and 16.78% ± 3.97%, respectively, compared with nonspecific TRPV3 inhibitor ruthenium red (20 μM), which had little rescue effect on cell death (Fig. 5, A and B).

Since forsythoside B was able to reduce the cytotoxicity of cells heterologously expressing the gain-of-function TRPV3 mutant, we further tested whether forsythoside B had any protective effect on HaCaT cells that originated from human keratinocytes. As shown in Fig. 5, C and D, the cell death ratio increased significantly in HaCaT cells transfected with the G573S mutant for 12 hours compared with normal HaCaT cells ($n = 4$, $P < 0.0001$). Adding nonspecific TRPV3 inhibitor ruthenium red at 20 μM had no rescue effect on cell death. In contrast, 100 μM forsythoside B partially reduced cell death ($P < 0.05$). Our results indicate that inhibition of TRPV3 by forsythoside B can attenuate cell death induced by overactive TRPV3 in both HEK293 cells and human HaCaT cells.

Forsythoside B Reduces Cytotoxicity Induced by Carvacrol in Both HEK293 Cells Expressing TRPV3 and HaCaT Cells. Atopic dermatitis is a feature of cell death

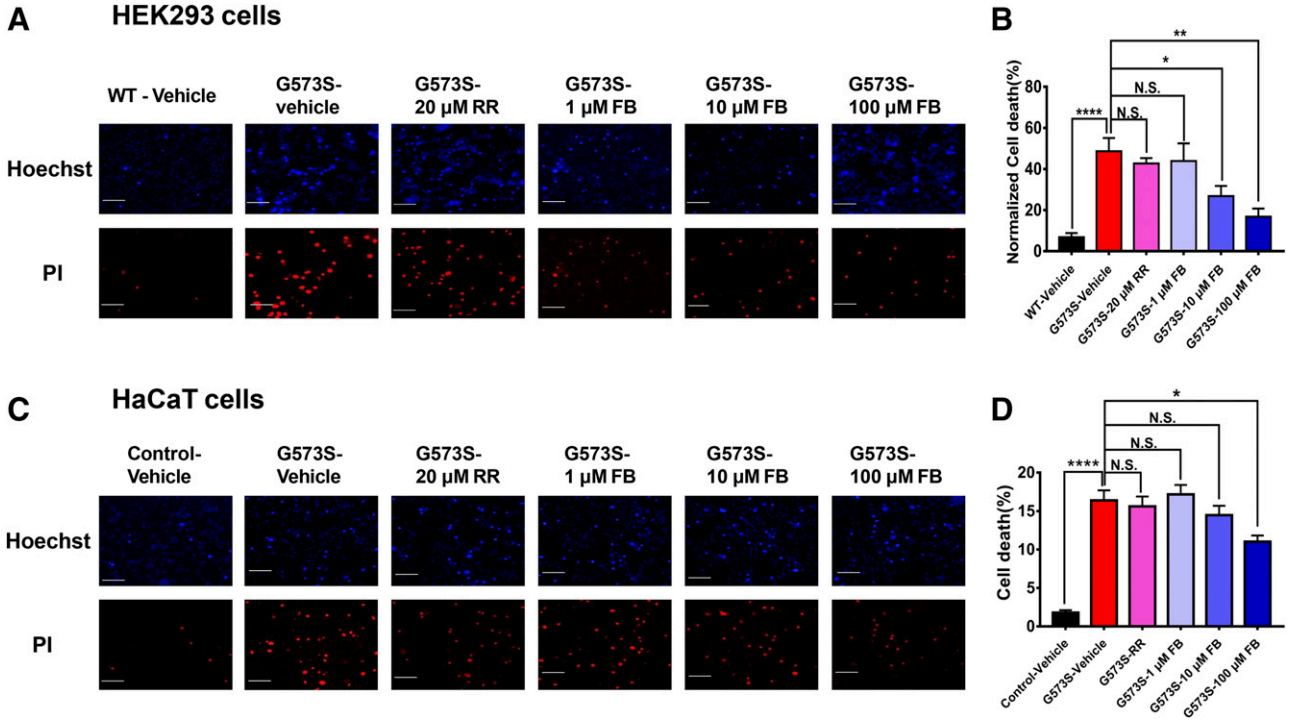

Fig. 5. Forsythoside B reduces cell death of HEK 293 cells and HaCaT cells expressing the gain-of-function TRPV3 G573S mutant. (A) Forsythoside B reduced the death of HEK293 cells expressing the TRPV3 G573S mutant in a dose-dependent manner. Representative Hoechst staining of cell nuclei (top images) and PI staining for dead cells (bottom images). Scale bar, 100 μm. (B) Statistical analysis for normalized cell death from (A). Five independent experiments were performed. Data are presented as means ± S.E.M. (C) Forsythoside B reduced the death of HaCaT cells expressing the TRPV3 G573S mutant in a dose-dependent manner. (D) Summary of the bar graph for (C). Four independent experiments were performed. Data are presented as means ± S.E.M. *$P < 0.05$; **$P < 0.01$; ****$P < 0.0001$. FB, forsythoside B; RR, ruthenium red

in keratinocytes, and pharmacological activation of TRPV3 by its agonist monoterpenoid carvacrol can also induce cell death in normal human epidermal keratinocyte cells (Szöllősi et al., 2018). To further confirm the specific inhibition of TRPV3 by forsythoside B, we tested the inhibitory effect of forsythoside B on TRPV3 current activated by 300 μM carvacrol in HEK293 cells expressing TRPV3. As shown in Fig. 6, A and B, forsythoside B dose-dependently inhibited TRPV3 current. We also further tested the rescue effect of forsythoside B on cell death in HEK293 cells expressing WT TRPV3 and human HaCaT cells. In HEK293 cells expressing WT TRPV3, 12 hours of 300 μM carvacrol treatment caused significant cell death (23.3% ± 2.59%; Fig. 6, C and D). Addition of 10 and 100 μM forsythoside B effectively reduced the cell death ratio to 12.83% ± 1.48% and 11.66% ± 1.32%, respectively. Compared with forsythoside B, ruthenium red also had a partial rescue effect on cell death. Interestingly, 300 μM carvacrol was unable to induce cell death in normal HEK293 cells, suggesting that carvacrol-induced cytotoxicity is dependent on the presence of TRPV3.

Similarly, the cell death ratio increased significantly in HaCaT cells treated with 300 μM carvacrol for 12 hours (Fig. 6, E and F). Treatment of HaCaT cells with forsythoside B caused a reduction in cell death, consistent with the results obtained from HEK293 cells (Fig. 6D). Our results indicate that pharmacological inhibition of TRPV3 by forsythoside B can reduce the cytotoxicity triggered by agonists in cells expressing TRPV3 channels.

Putative Binding Sites by Docking of Forsythoside B into the Cryo-Electron Microscopy Structure of Mouse TRPV3. The cryo-electron microscopy structure of a full-length mouse TRPV3 in both the apo closed state and the agonist-bound open state was recently solved at 4.3 Å (Singh et al., 2018). Based on the structure, we attempted

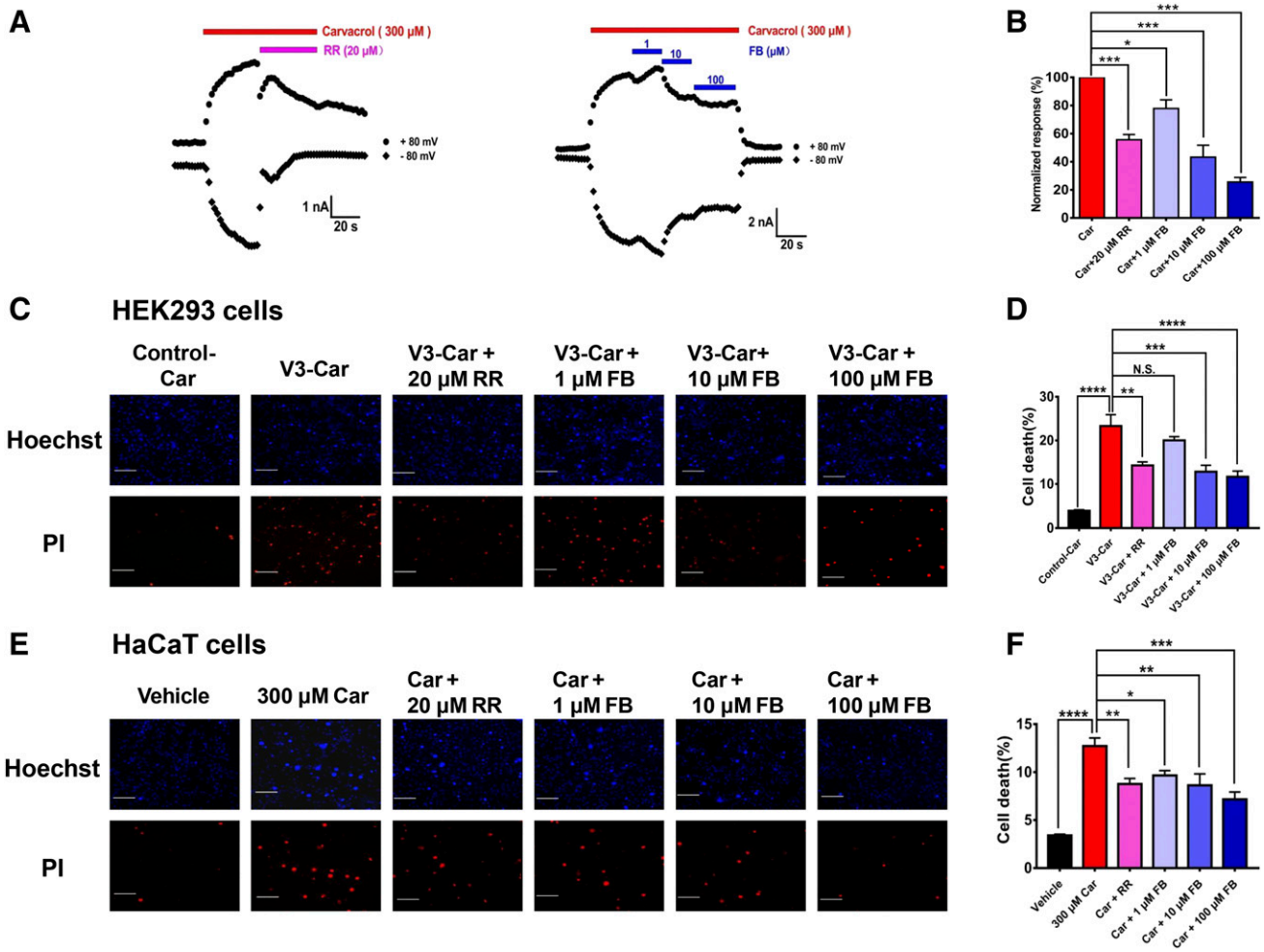

Fig. 6. Forsythoside B attenuates cell death in HEK293 cells expressing TRPV3 channels or HaCaT cells activated by TRPV3 agonist carvacrol. (A) The left panel shows the representative hTRPV3 current in response to 300 μM carvacrol (red bar) before and after its coaddition with ruthenium red (pink bar). The right panel shows the representative hTRPV3 current activated by 300 μM carvacrol (red bar) in the absence or presence of forsythoside B from 1 to 100 μM (blue bar) and washout. (B) A summary of TRPV3 current in response to different compounds in (A) (n = 6; by one-way analysis of variance). (C) Cell death assay after transient transfection with WT TRPV3 and after treatment with different compounds for 12 hours in HEK293 cells. (D) Summary of the cell death ratio after treatment with different compounds (n = 4). (E) Cell death assay after treatment with different compounds for 12 hours in HaCaT cells. (F) Summary of the cell death ratio after treatment with different compounds (n = 4). Data are presented as means ± S.E.M. *$P < 0.05$; **$P < 0.01$; ***$P < 0.001$; ****$P < 0.0001$. Car, carvacrol; FB, forsythoside B; N.S., no significance; RR, ruthenium red. Scale bar, 100 μm in (C) and (E).

to explore where and how compound forsythoside B binds to and causes inhibition of TRPV3 channel function. To identify the potential TRPV3 binding sites for forsythoside B, we used the AutoDock 4.2 program to dock forsythoside B into the mouse TRPV3 structure (Fig. 7, A and B). Our docking results showed a putative binding pocket for forsythoside B that was formed by residues T636 from the pore helix and F666 from S6 of one subunit and G638 and L639 from the selectivity filter of the neighboring subunit (Fig. 7C). As a result, forsythoside B inhibited TRPV3 channel activity by binding to the region between the selectivity filter and the central cavity of TRPV3 (Fig. 7D), thus likely making ions impermeable for passing through the intracellular gate of TRPV3 (Singh et al., 2018). Nevertheless, this binding site needs to be further validated by site-directed mutagenesis.

Discussion

In this study, our purpose was to identify a specific TRPV3 inhibitor as a tool that can be used to validate TRPV3 as a therapeutic target for treatment of chronic pruritus and dermatitis-related skin diseases. Using the calcium fluorescent assay in multiplate reader format, we screened and identified a natural compound (forsythoside B) that attenuates itch-scratching behavior and reduces cell death caused by overactive TRPV3. Our findings demonstrate that specific inhibition of TRPV3 by natural forsythoside B may present a promising treatment for chronic pruritus and inflammation-related skin diseases.

Accumulating evidence suggests that the warm temperature–sensitive and calcium-permeable TRPV3 channel plays a pivotal role in itch sensation, skin physiology, and pathology (Wang and Wang, 2017), although other thermo-TRP channels are reported to be involved in itch signaling (Zhang, 2015). The most convincing evidence for TRPV3 as a novel target for pruritus comes from observations on spontaneous mutations of TRPV3 that cause dermatitis in rodents and from studies on human genetic gain-of-function mutations in patients with OS characterized by atopic dermatitis and intolerable itchiness (Imura et al., 2009; Yoshioka et al., 2009; Lin et al., 2012; Duchatelet et al., 2014; Eytan et al., 2014; Kariminejad et al., 2014; Choi et al., 2018). Silencing of TRPV3 reduces itch-scratching behavior in mice (Yamamoto-Kasai et al., 2012). Conversely, pharmacological activation of TRPV3 by the natural pruritogen carvacrol induces scratching, whereas carvacrol-mediated itching is significantly attenuated in TRPV3 knockout mice (Cui et al., 2018). These lines of accumulated evidence indicate the critical role of TRPV3 in pruritus.

Natural compound forsythoside B is also an active ingredient in the fruit of *Forsythia suspensa*, which exhibits potent pharmacological antipyretic and anti-inflammatory activity (Muluye et al., 2014). *F. suspensa* extracts can suppress the release of inflammatory mediators, such as nitric oxide and proinflammatory cytokines prostaglandin E2, and can also

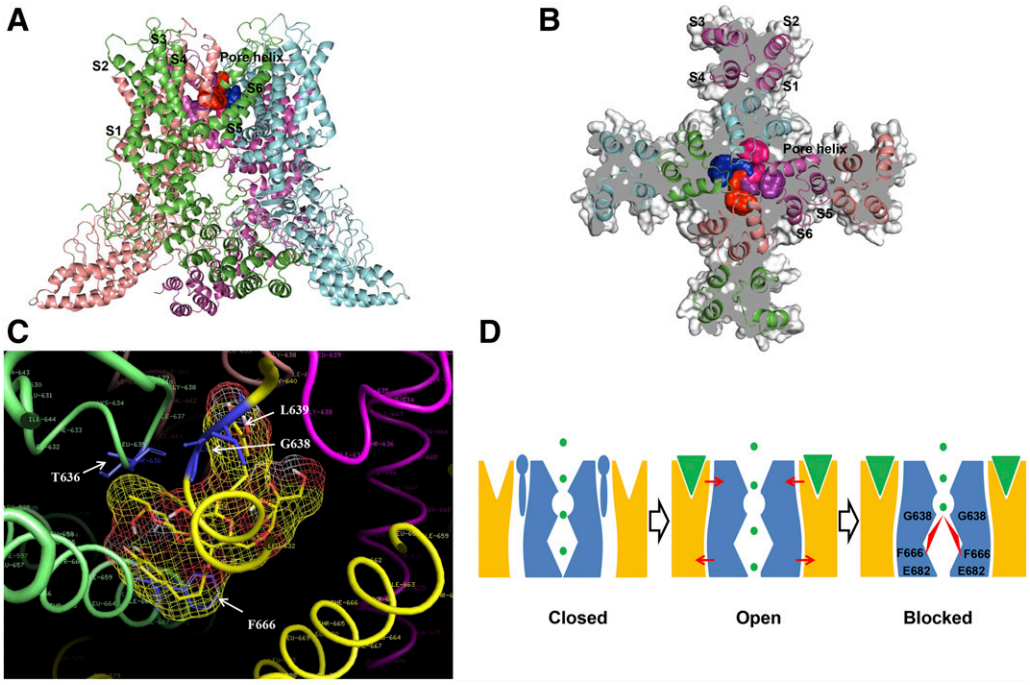

Fig. 7. Putative binding pocket for forsythoside B bound to the central cavity of mouse TRPV3. (A) Representative view of a coronal section for forsythoside B bound to the structure of TRPV3 subunits labeled in different colors of green, pink, purple, and cyan for each subunit. Four forsythoside B molecules bound to the binding pocket are also labeled in different colors of red, blue, purple, and hot pink. (B) Top view of four forsythoside B molecules bound to the TRPV3 structure. (C) Expanded view of putative binding sites of forsythoside B in TRPV3. Different subunits of TRPV3 are shown in different colors, and forsythoside B is shown in yellow mesh. The surrounding residues T636 from the pore helix and F666 from S6 of one subunit in green and G638 and L639 from the selectivity filter of the neighboring subunit in yellow are shown as blue sticks and indicated by white arrows. (D) Schematic diagram illustrating inhibition of TRPV3 by forsythoside B based on the model proposed by Singh et al. (2018). (Left) Putative lipids (blue) are located between the S1–S4 (orange) and S5 to S6 (blue) domains in the closed state. (Middle) Open TRPV3 upon binding of agonist 2-APB (in green triangles) to the top of S1–S4 domains, bringing the S1–S4 and pore domains close together. (Right) Forsythoside B (in red) binds to the putative pocket formed by residues from S6 and pore helices of TRPV3, thus blocking the region right below the selectivity filter and the central cavity.

reduce the level of inflammatory factors such as tumor necrosis factor-α and interleukin-6 (Lee et al., 2010, 2011). Forsythoside B also decreases endothelin-1 (another pruritogen) secretion and cyclooxygenase-2 activity and inhibits NF-κB signaling to exert its anti-inflammatory effects (Sahpaz et al., 2002; Martin-Nizard et al., 2004; Jiang et al., 2010a). In this study, our findings reveal a previously unknown mechanism of action for forsythoside B that inhibits the TRPV3 channel, which may help explain its broad anti-inflammatory effects. Forsythoside B can also be used as a tool to further validate TRPV3 as a therapeutic target for skin diseases such as atopic dermatitis or chronic pruritus.

In this study, we proposed a mechanism underlying the causative role of overactive TRPV3 in itch sensation and cytotoxicity of keratinocytes. Overactive TRPV3 induced by gain-of-function G573S mutation or pharmacological activation by the pruritogen carvacrol causes an excessive influx of calcium in keratinocytes (Fig. 8). Calcium influx activates calcineurin, which dephosphorylates the nuclear factor of activated T cells and induces translocation of the nuclear factor of activated T cells from the cytosol to the nucleus for promotion of thymic stromal lymphopoietin transcription and secretion (Wilson et al., 2013; Yamamoto-Kasai et al., 2013). TRPV3 activation also causes the release of histamine in the skin (Asakawa et al., 2006). Thymic stromal lymphopoietin, histamine, and cytokines released from keratinocytes stimulate afferent nerve endings that transmit the itch signal to the central nervous system via the dorsal horn of the spinal cord, thus evoking scratching behavior (Wilson et al., 2013; Bautista et al., 2014). For overactive TRPV3-mediated cytotoxicity, calcium overload results in keratinocyte cell death and keratinization or skin diseases via activation of an unidentified Ca^{2+}-dependent kinase (Fig. 8) (Xiao et al., 2008; Cao et al., 2012; Lin et al., 2012). Pharmacological inhibition of TRPV3 by forysthoside B, which likely binds to the region between the selectivity filter and the central cavity, attenuates itch signaling and cytotoxicity. However, detailed mechanisms of how TRPV3 activation induces the increase of histamine and how the excessive influx of calcium triggers cell death remain to be further investigated.

In summary, we identified a novel TRPV3 inhibitor (natural forsythoside B) that attenuates both acute and chronic itch by inhibition of TRPV3 channel function. Forsythoside B reduces cytotoxicity caused by either gain-of-function TRPV3 mutation or the channel agonist carvacrol. Therefore, natural compound forsythoside B may be beneficial for the treatment of pruritus and keratinocyte toxicity-related skin inflammation and diseases.

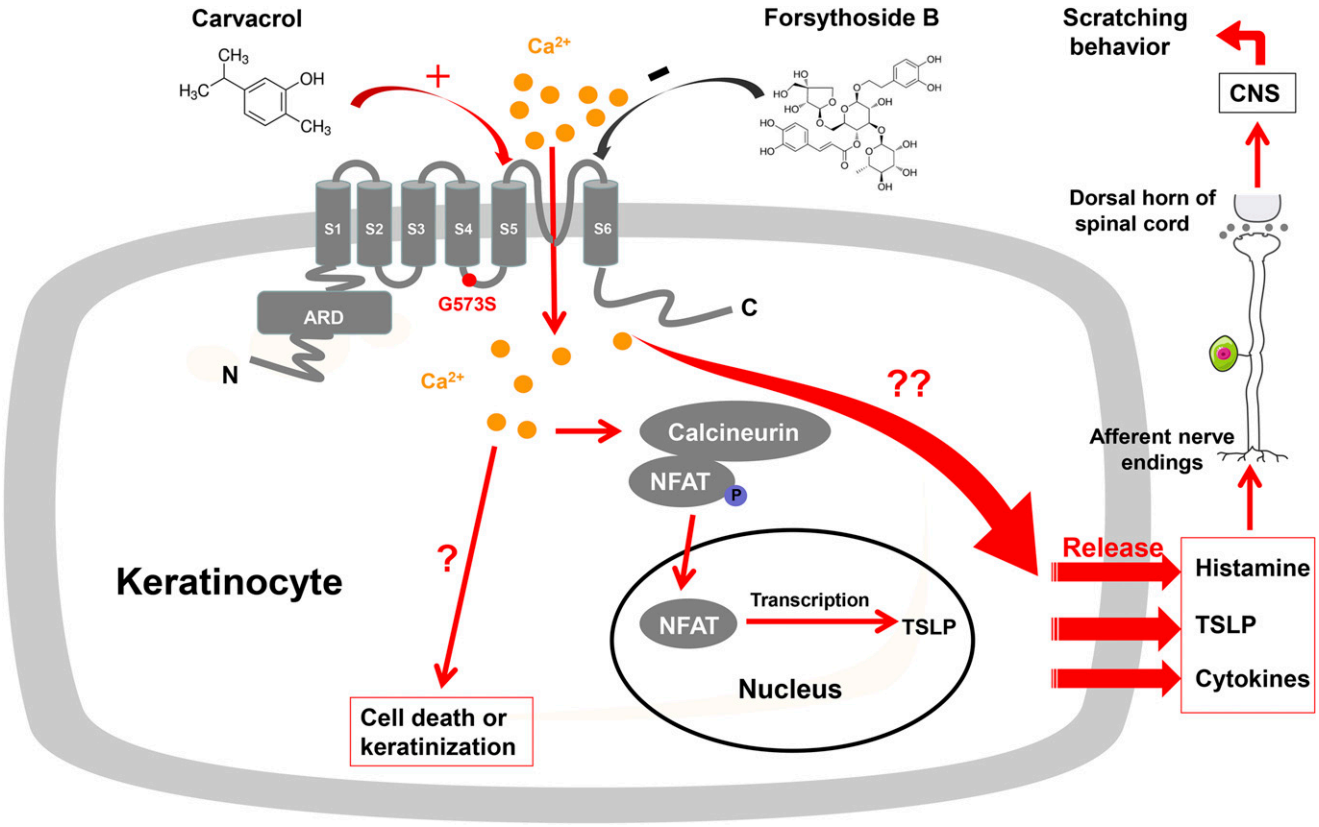

Fig. 8. Proposed mechanism for the causative role of overactive TRPV3 in itch signaling and cytotoxicity of keratinocytes. For TRPV3-mediated itch signaling, activation of TRPV3 by channel agonist carvacrol or gain-of-function mutation results in an elevation of intracellular calcium that leads to the activation of calcineurin. Calcineurin dephosphorylates NFAT and induces the translocation of NFAT from the cytosol to the nucleus. Translocation of NFAT induces TSLP transcription and thus promotes TSLP secretion in the keratinocytes. TSLP, histamine, and cytokines released by TRPV3 activation stimulate the afferent nerve endings that transmit the itch signal through the dorsal horn of the spinal cord to the CNS to evoke scratching behavior. For overactive TRPV3-mediated cytotoxicity, the excessive influx of calcium induces keratinocyte cell death via activation of an unidentified Ca^{2+}-dependent kinase. ARD, ankyrin repeat domain; CNS, central nervous system; NFAT, nuclear factor of activated T cells; TSLP, thymic stromal lymphopoietin.

Acknowledgments

We thank Alexander I. Sobolevsky for kindly providing the Protein Data Bank files of mouse TRPV3 structures and Dr. Zhun Wei and Dr. Changdong Liu for help with molecular docking.

Authorship Contributions

Participated in research design: Zhang, Sun, K. Wang.
Conducted experiments: Zhang, Sun, Qi, Ma.
Contributed new reagents or analytic tools: Zhou, W. Wang.
Performed data analysis: Zhang, Sun.
Wrote or contributed to the writing of the manuscript: Zhang, Sun, K. Wang.

References

Aijima R, Wang B, Takao T, Mihara H, Kashio M, Ohsaki Y, Zhang JQ, Mizuno A, Suzuki M, Yamashita Y, et al. (2015) The thermosensitive TRPV3 channel contributes to rapid wound healing in oral epithelia. *FASEB J* **29**:182–192.
Asakawa M, Yoshioka T, Matsutani T, Hikita I, Suzuki M, Oshima I, Tsukahara K, Arimura A, Horikawa T, Hirasawa T, et al. (2006) Association of a mutation in TRPV3 with defective hair growth in rodents. *J Invest Dermatol* **126**:2664–2672.
Bang S, Yoo S, Yang TJ, Cho H, and Hwang SW (2010) Farnesyl pyrophosphate is a novel pain-producing molecule via specific activation of TRPV3. *J Biol Chem* **285**: 19362–19371.
Bang S, Yoo S, Yang TJ, Cho H, and Hwang SW (2011) Isopentenyl pyrophosphate is a novel antinociceptive substance that inhibits TRPV3 and TRPA1 ion channels. *Pain* **152**:1156–1164.
Bang S, Yoo S, Yang TJ, Cho H, and Hwang SW (2012) 17(R)-resolvin D1 specifically inhibits transient receptor potential ion channel vanilloid 3 leading to peripheral antinociception. *Br J Pharmacol* **165**:683–692.
Bautista DM, Wilson SR, and Hoon MA (2014) Why we scratch an itch: the molecules, cells and circuits of itch. *Nat Neurosci* **17**:175–182.
Cao X, Yang F, Zheng J, and Wang K (2012) Intracellular proton-mediated activation of TRPV3 channels accounts for the exfoliation effect of α-hydroxyl acids on keratinocytes. *J Biol Chem* **287**:25905–25916.
Chen Y, Fang Q, Wang Z, Zhang JY, MacLeod AS, Hall RP, and Liedtke WB (2016) Transient receptor potential vanilloid 4 ion channel functions as a pruriceptor in epidermal keratinocytes to evoke histaminergic itch. *J Biol Chem* **291**: 10252–10262.
Cheng X, Jin J, Hu L, Shen D, Dong XP, Samie MA, Knoff J, Eisinger B, Liu ML, Huang SM, et al. (2010) TRP channel regulates EGFR signaling in hair morphogenesis and skin barrier formation. *Cell* **141**:331–343.
Choi JY, Kim SE, Lee SE, and Kim SC (2018) Olmsted syndrome caused by a heterozygous p.Gly568Val missense mutation in TRPV3 gene. *Yonsei Med J* **59**: 341–344.
Chung MK, Güler AD, and Caterina MJ (2005) Biphasic currents evoked by chemical or thermal activation of the heat-gated ion channel, TRPV3. *J Biol Chem* **280**: 15928–15941.
Chung MK, Lee H, Mizuno A, Suzuki M, and Caterina MJ (2004) 2-aminoethoxydiphenyl borate activates and sensitizes the heat-gated ion channel TRPV3. *J Neurosci* **24**:5177–5182.
Cui TT, Wang GX, Wei NN, and Wang K (2018) A pivotal role for the activation of TRPV3 channel in itch sensations induced by the natural skin sensitizer carvacrol. *Acta Pharmacol Sin* **39**:331–335.
Duchatelet S, Pruvost S, de Veer S, Fraitag S, Nitschké P, Bole-Feysot C, Bodemer C, and Hovnanian A (2014) A new TRPV3 missense mutation in a patient with Olmsted syndrome and erythromelalgia. *JAMA Dermatol* **150**:303–306.
Eytan O, Fuchs-Telem D, Mevorach B, Indelman M, Bergman R, Sarig O, Goldberg I, Adir N, and Sprecher E (2014) Olmsted syndrome caused by a homozygous recessive mutation in TRPV3. *J Invest Dermatol* **134**:1752–1754.
Imura K, Yoshioka T, Hirasawa T, and Sakata T (2009) Role of TRPV3 in immune response to development of dermatitis. *J Inflamm (Lond)* **6**:17.
Jiang WL, Fu FH, Xu BM, Tian JW, Zhu HB, and Jian-Hou (2010a) Cardioprotection with forsythoside B in rat myocardial ischemia-reperfusion injury: relation to inflammation response. *Phytomedicine* **17**:635–639.
Jiang WL, Tian JW, Fu FH, Zhu HB, and Hou J (2010b) Neuroprotective efficacy and therapeutic window of forsythoside B: in a rat model of cerebral ischemia and reperfusion injury. *Eur J Pharmacol* **640**:75–81.
Jiang WL, Yong-Xu, Zhang SP, Zhu HB, and Jian-Hou (2012) Forsythoside B protects against experimental sepsis by modulating inflammatory factors. *Phytother Res* **26**: 981–987.
Kariminejad A, Barzegar M, Abdollahimajd F, Pramanik R, and McGrath JA (2014) Olmsted syndrome in an Iranian boy with a new de novo mutation in TRPV3. *Clin Exp Dermatol* **39**:492–495.
Lee JY, Cho BJ, Park TW, Park BE, Kim SJ, Sim SS, and Kim CJ (2010) Dibenzylbutyrolactone lignans from Forsythia koreana fruits attenuate lipopolysaccharide-induced inducible nitric oxide synthetase and cyclooxygenase-2 expressions through activation of nuclear factor-κb and mitogen-activated protein kinase in RAW264.7 cells. *Biol Pharm Bull* **33**:1847–1853.
Lee S, Shin S, Kim H, Han S, Kim K, Kwon J, Kwak JH, Lee CK, Ha NJ, Yim D, et al. (2011) Anti-inflammatory function of arctiin by inhibiting COX-2 expression via NF-κB pathways. *J Inflamm (Lond)* **8**:16.
Lin Z, Chen Q, Lee M, Cao X, Zhang J, Ma D, Chen L, Hu X, Wang H, Wang X, et al. (2012) Exome sequencing reveals mutations in TRPV3 as a cause of Olmsted syndrome. *Am J Hum Genet* **90**:558–564.
Luo J, Stewart R, Berdeaux R, and Hu H (2012) Tonic inhibition of TRPV3 by Mg^{2+} in mouse epidermal keratinocytes. *J Invest Dermatol* **132**:2158–2165.
Martin-Nizard F, Sahpaz S, Kandoussi A, Carpentier M, Fruchart JC, Duriez P, and Bailleul F (2004) Natural phenylpropanoids inhibit lipoprotein-induced endothelin-1 secretion by endothelial cells. *J Pharm Pharmacol* **56**:1607–1611.
Miyamoto T, Nojima H, Shinkado T, Nakahashi T, and Kuraishi Y (2002) Itch-associated response induced by experimental dry skin in mice. *Jpn J Pharmacol* **88**:285–292.
Morris GM, Goodsell DS, Halliday RS, Huey R, Hart WE, Belew RK, and Olson AJ (1998) Automated docking using a Lamarckian genetic algorithm and an empirical binding free energy function. *J Comput Chem* **19**:1639–1662.
Muluye RA, Bian Y, and Alemu PN (2014) Anti-inflammatory and antimicrobial effects of heat-clearing Chinese herbs: a current review. *J Tradit Complement Med* **4**:93–98.
Nilius B, Owsianik G, Voets T, and Peters JA (2007) Transient receptor potential cation channels in disease. *Physiol Rev* **87**:165–217.
Sahpaz S, Garbacki N, Tits M, and Bailleul F (2002) Isolation and pharmacological activity of phenylpropanoid esters from Marrubium vulgare. *J Ethnopharmacol* **79**: 389–392.
Schüttelkopf AW and van Aalten DM (2004) PRODRG: a tool for high-throughput crystallography of protein-ligand complexes. *Acta Crystallogr D Biol Crystallogr* **60**:1355–1363.
Sherkheli MA, Gisselmann G, and Hatt H (2012) Supercooling agent icilin blocks a warmth-sensing ion channel TRPV3. *Sci World J* **2012**:982725.
Singh AK, McGoldrick LL, and Sobolevsky AI (2018) Structure and gating mechanism of the transient receptor potential channel TRPV3. *Nat Struct Mol Biol* **25**: 805–813.
Sun S and Dong X (2016) Trp channels and itch. *Semin Immunopathol* **38**:293–307.
Sun XY, Sun LL, Qi H, Gao Q, Wang GX, Wei NN, and Wang K (2018) Antipruritic effect of natural coumarin osthole through selective inhibition of thermosensitive TRPV3 channel in the skin. *Mol Pharmacol* **94**:1164–1173.
Szöllősi AG, Vasas N, Angyal Á, Kistamás K, Nánási PP, Mihály J, Béke G, Herczeg-Lisztes E, Szegedi A, Kawada N, et al. (2018) Activation of TRPV3 regulates inflammatory actions of human epidermal keratinocytes. *J Invest Dermatol* **138**: 365–374.
Wang G and Wang K (2017) The Ca^{2+}-permeable cation transient receptor potential TRPV3 channel: an emerging pivotal target for itch and skin diseases. *Mol Pharmacol* **92**:193–200.
Wei NN, Lv HN, Wu Y, Yang SL, Sun XY, Lai R, Jiang Y, and Wang K (2016) Selective activation of nociceptor TRPV1 channel and reversal of inflammatory pain in mice by a novel coumarin derivative Muralatin L from Murraya alata. *J Biol Chem* **291**:640–651.
Wilson SR, Thé L, Batia LM, Beattie K, Katibah GE, McClain SP, Pellegrino M, Estandian DM, and Bautista DM (2013) The epithelial cell-derived atopic dermatitis cytokine TSLP activates neurons to induce itch. *Cell* **155**:285–295.
Xiao R, Tian J, Tang J, and Zhu MX (2008) The TRPV3 mutation associated with the hairless phenotype in rodents is constitutively active. *Cell Calcium* **43**:334–343.
Xu H, Delling M, Jun JC, and Clapham DE (2006) Oregano, thyme and clove-derived flavors and skin sensitizers activate specific TRP channels. *Nat Neurosci* **9**: 628–635.
Yamamoto-Kasai E, Imura K, Yasui K, Shichijou M, Oshima I, Hirasawa T, Sakata T, and Yoshioka T (2012) TRPV3 as a therapeutic target for itch. *J Invest Dermatol* **132**:2109–2112.
Yamamoto-Kasai E, Yasui K, Shichijo M, Sakata T, and Yoshioka T (2013) Impact of TRPV3 on the development of allergic dermatitis as a dendritic cell modulator. *Exp Dermatol* **22**:820–824.
Yoshioka T, Imura K, Asakawa M, Suzuki M, Oshima I, Hirasawa T, Sakata T, Horikawa T, and Arimura A (2009) Impact of the Gly573Ser substitution in TRPV3 on the development of allergic and pruritic dermatitis in mice. *J Invest Dermatol* **129**:714–722.
Zhang X (2015) Targeting TRP ion channels for itch relief. *Naunyn Schmiedebergs Arch Pharmacol* **388**:389–399.
Zhu B, Gong N, Fan H, Peng CS, Ding XJ, Jiang Y, and Wang YX (2014) Lamiophlomis rotata, an orally available Tibetan herbal painkiller, specifically reduces pain hypersensitivity states through the activation of spinal glucagon-like peptide-1 receptors. *Anesthesiology* **121**:835–851.

Address correspondence to: KeWei Wang, Department of Pharmacology, School of Pharmacy, Qingdao University, 38 Dengzhou Rd., Qingdao 266021, China. E-mail: wangkw@qdu.edu.cn